

Karbala International Journal of Modern Science

Manuscript 3327

Dyadosphere Space-Time of a Charged Black Hole in the Rainbow Gravity and Energy Distribution

Oktay Aydogdu

Mustafa Salti

Follow this and additional works at: <https://kijoms.uokerbala.edu.iq/home>



Part of the [Physics Commons](#)



Dyadosphere Space-Time of a Charged Black Hole in the Rainbow Gravity and Energy Distribution

Abstract

One is prompted to examine an energy-dependent space-time with significant distortion of standard general relativity through a breach of the Lorentz invariance in high-energy quantum gravity. The present study explores how the energy of a test particle influences the energy density of a charged black hole in the framework of rainbow gravity. In this context, the focus is on investigating the dyadosphere of the black hole, where the space-time fabric is influenced by the energy of the test particle. We also employ graphical analysis to visually illustrate the variations in the black hole's energy density defined within the framework of the quantum gravity perspective.

Keywords

Gravity's rainbow; Rainbow function; Dyadosphere; Black hole; Energy density.

Creative Commons License



This work is licensed under a [Creative Commons Attribution-Noncommercial-No Derivative Works 4.0 License](https://creativecommons.org/licenses/by-nc-nd/4.0/).

RESEARCH PAPER

Dyadosphere Space-time of a Charged Black Hole in the Rainbow Gravity and Energy Distribution

Oktay Aydogdu*, Mustafa Salti

Department of Physics, Faculty of Science, Mersin University, Mersin, Turkey

Abstract

One is prompted to examine an energy-dependent space-time with significant distortion of standard general relativity through a breach of the Lorentz invariance in high-energy quantum gravity. The present study explores how the energy of a test particle influences the energy density of a charged black hole in the framework of rainbow gravity. In this context, the focus is on investigating the dyadosphere of the black hole, where the space-time fabric is influenced by the energy of the test particle. We also employ graphical analysis to visually illustrate the variations in the black hole's energy density defined within the framework of the quantum gravity perspective.

Keywords: Gravity's rainbow, Rainbow function, Dyadosphere, Black hole, Energy density

1. Introduction

How to conciliate gravity with quantum principles is perhaps the most challenging theoretical question confronting science in the twenty-first century. The solution to this problem, which is expected to encompass a description of quantum space-time, should serve as the fundamental cornerstone for the rest of physics. Regrettably, despite the concerted efforts of numerous scientists, a quantum theory of gravity has yet to be developed. Nevertheless, it is an important theoretical accomplishment in this pursuit that we have candidate theories capable of explaining various physical phenomena, as we strive to construct a comprehensive quantum theory of gravity [1–7]. One such theory is the rainbow formalism of general relativity (RFGR), which takes into account the quantum mechanical effects on particles in curved space-time. It can be argued that the emergence of the RFGR is driven by two main factors. One of them is that Einstein's theory of gravity performs well in the infrared (IR) range but fulfills poorly in the ultraviolet (UV) range. This is because the energy-

momentum dispersion relation, which maintains Lorentz invariance in the IR region, fails to preserve this symmetry in the UV region within the framework of the general relativity theory [8]. As a means to address this issue, doubly special relativity (DSR) takes the Planck energy and speed of light as upper bounds and operates in the minimum accessible region dominated by the effect of quantum gravity [9]. In the context of DSR, $\mathcal{F}_1(\varepsilon)$ and $\mathcal{F}_2(\varepsilon)$ should satisfy the following modified dispersion relation at the Planck scale in order to preserve the energy-momentum invariance

$$\mathcal{F}_1^2(\varepsilon)E^2 = \mathcal{F}_2^2(\varepsilon)p^2 + m^2, \quad (1)$$

where $\mathcal{F}_1(\varepsilon)$ and $\mathcal{F}_2(\varepsilon)$ are rainbow functions that rely on the properties of the space-time curvature. Here, ε is defined in terms of the test particle (E_{PR}) and Planck (E_{PL}) energies as $\varepsilon = E_{PR}E_{PL}^{-1}$. It is worth noting that the relation expressed in Equation (1) can be reduced to the known energy-momentum dispersion under the low-energy limit $\lim_{\varepsilon \rightarrow 0} \mathcal{F}_i(\varepsilon) = 1$, where $i = 1, 2$, which is known as the correspondence principle of the RFGR [10]. Emphasizing the significance of the choice of rainbow function, it is

Received 26 May 2023; revised 8 August 2023; accepted 15 August 2023.
Available online 12 October 2023

* Corresponding author.
E-mail addresses: oktaydogdu@mersin.edu.tr (O. Aydogdu), msalti@mersin.edu.tr (M. Salti).

<https://doi.org/10.33640/2405-609X.3327>

2405-609X/© 2023 University of Kerbala. This is an open access article under the CC-BY-NC-ND license (<http://creativecommons.org/licenses/by-nc-nd/4.0/>).

essential to recognize that it profoundly influences the examination of the studied physical quantity, rendering this selection phenomenologically relevant and motivating. For instance, the $\mathcal{F}_1(\varepsilon) = 1$ and $\mathcal{F}_2(\varepsilon) = 1 + \varepsilon/2$ forms of rainbow functions were used to investigate the geodesic structure of the Schwarzschild black hole [11]. The other reason is that space-time should be characterized using an energy-dependent metric when gravity arises from quantum degrees of freedom. To deal with this, Magueijo and Smolin extended doubly special relativity into curved space-time, giving rise to the rainbow formalism of general relativity (RFGR) [12]. According to this novel formalism, particles can receive energy by interacting with space-time, resulting in different trajectories within the same gravitational field [10,12]. Furthermore, modifying the energy distribution of particles can have a significant impact on the behavior of matter near black holes and other objects with strong gravitational fields. Therefore, the RFGR serves as a crucial tool for investigating and advancing our comprehension of fundamental physical laws, encompassing quantum mechanics and general relativity. Thenceforth, the RFGR as a quantum gravity perspective has been utilized to explore various physical properties of black holes, including the geodesic structure [11], entropy [13–15], thermodynamics [16–20], thermodynamic phase transition [21], Hawking radiation [22,23], effective horizon [24], complementarity [25], and initial singularity problem [26].

On the one hand, it is well established that black holes provide fertile ground for studying quantum gravity, as demonstrated by Hawking's discovery in the 1970s that black holes can emit matter and radiation within the framework of quantum mechanics [27]. Furthermore, attaining a thorough comprehension of black holes could serve as a crucial milestone in advancing the theory of quantum gravity. On the other hand, exploring the energy distribution of black holes can provide insights into their formation, evolution, environment, and quantum properties, while also having practical applications in astrophysics and cosmology. So far, the topic of black hole energy density has exclusively been examined within the framework of either the general theory of relativity or its modified theories. However, it is widely acknowledged that all of these theories adopt a classical perspective. In this context, it is obvious that discussing the energy distributions of black holes in the RFGR, which is one of the most promising contenders in the realm of quantum gravity theory, will yield remarkable outcomes. To achieve this objective, the dyadosphere configuration of an electromagnetic black

hole, proposed in [28–30] as a suitable approach for elucidating gamma radiation bursts, is considered.

The subsequent sections are structured as follows. In the second section, the space-time form is composed in the RFGR. The third section is devoted to computing the energy density of the dyadosphere of a charged black hole in the RFGR. Graphical analyses and discussion are presented in the fourth section. Closing remarks are given in the last section.

G , \hbar , and c are taken equal to unity throughout the study. Moreover, the tensor indices and local Lorentz indices are represented by the Greek ($\alpha, \beta, \gamma \dots$) and Latin ($a, b, c \dots$) letters, respectively.

2. Space-time in the RFGR

De Lorenci and colleagues have reconstructed the Reissner-Nordström space-time configuration, which was proposed to explain gamma-ray bursts occurring in charged black holes [28–30]. This reconstruction takes into consideration the first-order contributions of the Euler-Heisenberg Lagrangian and is outlined as follows [31].

$$ds^2 = \mathfrak{S}^2(r)dt^2 - \mathfrak{S}^{-2}(r)dr^2 - r^2d\theta^2 - r^2\sin^2\theta d\phi^2. \quad (2)$$

Here, $\mathfrak{S}^2(r) = 1 - \frac{2M}{r} + \frac{Q^2}{r^2} - \frac{\varsigma Q^4}{5r^6}$ where M and Q respectively indicate the mass and charge of the black hole while gravitational coupling constant for non-linear electrodynamics is represented by ς . Here are three significant aspects that should be taken into account in this context: i) if ς is extremely minuscule, the contribution of $\frac{\varsigma Q^4}{5r^6}$ can be disregarded; ii) the contribution of $\frac{\varsigma Q^4}{5r^6}$ is insignificant when $\frac{Q^2}{r^2} \gg \frac{\varsigma Q^4}{5r^6}$; iii) Equation (2) reduces to the standard Reissner-Nordström metric as ς is set to zero. In literature, wormholes [32], classical energy [33,34], and entropy [35] have been studied for the space-time given in Equation (2). On the other hand, as mentioned in the introduction, the RFGR alludes to the fact that space-time geometry switches energy, resulting in a distinct classical geometry for each energy quantum. This is manifested through the use of rainbow functions in the space-time metric [10,11]. Thus, considering the metric (2), one can achieve the following energy-dependent space-time model by chasing the method $dt \rightarrow \mathcal{F}_1^{-1}(\varepsilon)dt$ and $dx^i \rightarrow \mathcal{F}_2^{-1}(\varepsilon)dx^i$ introduced in [10,11] in view of the RFGR

$$ds^2 = \mathfrak{S}^2(r)\mathcal{F}_1^{-2}(\varepsilon)dt^2 - \mathfrak{S}^{-2}(r)\mathcal{F}_2^{-2}(\varepsilon)dr^2 - \mathcal{F}_2^{-2}(\varepsilon)r^2(d\theta^2 + \sin^2\theta d\phi^2). \quad (3)$$

So, the metric tensor and its inverse for the aforementioned space-time can be respectively expressed as

$$g_{\alpha\beta} = \mathfrak{N}^2 \mathcal{F}_1^{-2} \delta_\alpha^0 \delta_\beta^0 - \mathfrak{N}^{-2} \mathcal{F}_2^{-2} \delta_\alpha^1 \delta_\beta^1 - \mathcal{F}_2^{-2} r^2 \delta_\alpha^2 \delta_\beta^2 - \mathcal{F}_2^{-2} r^2 \sin^2 \theta \delta_\alpha^3 \delta_\beta^3, \quad (4)$$

$$g^{\alpha\beta} = \mathfrak{N}^{-2} \mathcal{F}_1^2 \delta_0^\alpha \delta_0^\beta - \mathfrak{N}^2 \mathcal{F}_2^2 \delta_1^\alpha \delta_1^\beta - \mathcal{F}_2^2 r^{-2} \delta_2^\alpha \delta_2^\beta - \mathcal{F}_2^2 r^{-2} \sin^{-2} \theta \delta_3^\alpha \delta_3^\beta. \quad (5)$$

3. Energy density

Our preference lies in computing the energy density of the charged black hole with a rainbow effect within the framework of teleparallel theory (TT), which describes gravitational interactions in terms of torsion rather than curvature [36]. The rationale behind this selection is that the TT offers a comparatively uncomplicated solution to the enduring problem of calculating energy within the framework of Einstein's general relativity (more comprehensive information can be found in [37–40]).

The gravitational energy-momentum tensor is given as follows [37].

$$\wp^{(a)} = \iiint (\partial_j X^{(a)j}) d^3x, \quad (6)$$

where gravitational energy density is expressed as

$$\chi = \partial_j X^{(a)j} = \partial_j \left(\frac{\det(H_\beta^{(i)})}{4\pi} \Xi^{(a)0j} \right), \quad (7)$$

and

$$\Xi^{(a)(b)(c)} = \frac{1}{4} (T^{(a)(b)(c)} + T^{(b)(a)(c)} - T^{(c)(a)(b)}) + \frac{1}{2} (\eta^{(ac)} T^{(b)} - \eta^{(ab)} T^{(c)}). \quad (8)$$

Here, the torsion tensor is defined in the following form [41].

$$T_{\alpha\beta}^{(j)} = \partial_\alpha h_\beta^{(j)} - \partial_\beta h_\alpha^{(j)}, \quad (9)$$

while

$$T^{(a)} = T_{(b)}^{(b)(a)}. \quad (10)$$

It should be noted that one can interchange the tensor indices with the local Lorentz indices using the tetrad tensor, or vice versa, that is $T^{(a)} = h_{(b)}^\alpha h_\beta^{(a)} g^{\beta\mu} T_{\alpha\mu}^{(b)}$. Moreover, the tetrad tensor $h_\beta^{(j)}$ which establishes a connection between flat and curved space-time, gives rise to the following relation

$$g_{\alpha\beta} = h_\alpha^{(i)} h_\beta^{(j)} \eta_{(ij)}, \quad (11)$$

where $\eta_{(ij)}$ indicates the Minkowski metric tensor.

The components of the tetrad for the energy-dependent metric (3) can be determined by introducing the general coordinate transformation $h_\alpha^{(j)} = \frac{\partial X^{\beta'}}{\partial X^\alpha} h_{\beta'}^{(j)}$ where $X^{\beta'}$ and X^α respectively represent the Schwarzschild and the isotropic coordinates (t, r, θ, ϕ) [37]:

$$h_\alpha^{(j)} = \mathfrak{N} \mathcal{F}_1^{-1} \delta_0^{(i)} \delta_\alpha^0 + \mathfrak{N}^{-1} \mathcal{F}_2^{-1} \sin \theta \left(\cos \phi \delta_1^{(i)} + \sin \phi \delta_2^{(i)} \right) \delta_\alpha^1 + \mathcal{F}_2^{-1} r \cos \theta \left(\cos \phi \delta_1^{(i)} + \sin \phi \delta_2^{(i)} \right) \delta_\alpha^2 + \mathcal{F}_2^{-1} r \sin \theta \left(-\sin \phi \delta_1^{(i)} + \cos \phi \delta_2^{(i)} \right), \quad (12)$$

$$h_\alpha^{(j)} = \mathfrak{N}^{-1} \mathcal{F}_1 \delta_0^{(i)} \delta_\alpha^0 + \mathfrak{N} \mathcal{F}_2 \sin \theta \left(\cos \phi \delta_1^{(i)} + \sin \phi \delta_2^{(i)} \right) \delta_\alpha^1 + \mathcal{F}_2 r^{-1} \cos \theta \left(\cos \phi \delta_1^{(i)} + \sin \phi \delta_2^{(i)} \right) \delta_\alpha^2 + \mathcal{F}_2 r^{-1} \sin \theta \left(\cos \phi \delta_2^{(i)} - \sin \phi \delta_1^{(i)} \right) \delta_\alpha^3, \quad (13)$$

where δ indicates the Kronecker delta function. The form of the non-zero elements of the torsion tensor (9) is acquired as follows

$$T_{01}^{(0)} = -T_{10}^{(0)} = -\mathcal{F}_1^{-1} \frac{d\mathfrak{N}}{dr}, \quad (14)$$

$$T_{12}^{(1)} = -T_{21}^{(1)} = \mathcal{F}_2^{-1} (1 - \mathfrak{N}^{-1}) \cos \theta \cos \phi, \quad (15)$$

$$T_{13}^{(1)} = -T_{31}^{(1)} = \mathcal{F}_2^{-1} (\mathfrak{N}^{-1} - 1) \sin \theta \sin \phi, \quad (16)$$

$$T_{12}^{(2)} = -T_{21}^{(2)} = \mathcal{F}_2^{-1} (1 - \mathfrak{N}^{-1}) \cos \theta \sin \phi, \quad (17)$$

$$T_{13}^{(2)} = -T_{31}^{(2)} = \mathcal{F}_2^{-1} (1 - \mathfrak{N}^{-1}) \sin \theta \cos \phi, \quad (18)$$

$$T_{12}^{(3)} = -T_{21}^{(3)} = \mathcal{F}_2^{-1} (\mathfrak{N}^{-1} - 1) \sin \theta. \quad (19)$$

Then, by utilizing Equations (14)–(19) along with Equations (8), (12) and (13), the necessary components of the $\Xi^{(a)0i}$ tensor required for computing the energy density are calculated as follows

$$\Xi^{(0)01} = \frac{\mathcal{F}_1 \mathcal{F}_2^2}{2} \left(\frac{d\mathfrak{N}}{dr} + \frac{2(\mathfrak{N} - 1)}{r} \right), \quad \Xi^{(0)02} = \Xi^{(0)03} = 0. \quad (20)$$

Consequently, the gravitational energy density for the dyadosphere of an energy-dependent

charged black hole (3) is achieved in the following form

$$\chi = \frac{\sin \theta}{8\pi\mathcal{F}_2} \left(\frac{\frac{4M}{r} - \frac{4Q^2}{r^2} + \frac{12Q^4\zeta}{5r^6}}{\sqrt{1 + \frac{Q^2}{r^2} - \frac{2M}{r} - \frac{Q^4\zeta}{5r^6}}} + \frac{\frac{3Q^2}{r^2} - \frac{2M}{r} - \frac{21Q^4\zeta}{5r^6}}{\sqrt{1 + \frac{Q^2}{r^2} - \frac{2M}{r} - \frac{Q^4\zeta}{5r^6}}} - \frac{\left(\frac{M}{r} - \frac{Q^2}{r^2} + \frac{3Q^4\zeta}{5r^6}\right)^2}{\left(1 + \frac{Q^2}{r^2} - \frac{2M}{r} - \frac{Q^4\zeta}{5r^6}\right)^{3/2}} + 2\sqrt{1 + \frac{Q^2}{r^2} - \frac{2M}{r} - \frac{Q^4\zeta}{5r^6}} - 2 \right). \quad (21)$$

In order to get an analytical expression for the gravitational energy, one can expand the energy density (21) up to the third-order as follow

$$\chi \approx \frac{\sin \theta}{8\pi\mathcal{F}_2} \left(\frac{2\sqrt{-Q^4\zeta}}{\sqrt{5}r^3} - 2 + \frac{3\sqrt{5}Q^2r}{\sqrt{-Q^4\zeta}} - \frac{12(\sqrt{5}M)r^2}{\sqrt{-Q^4\zeta}} + O[r]^3 \right), \quad (22)$$

which leads to the following gravitational energy

$$\wp^{(0)} = \frac{\sqrt{5}(3r^4(5Q^2 - 16Mr) - 8Q^4\zeta \text{Log}(r))}{160\mathcal{F}_2\sqrt{-Q^4\zeta}} - \frac{\pi r}{4\mathcal{F}_2}. \quad (23)$$

4. Discussion of results

The energy density, as shown in Equation (21), is dependent on several factors, including the charge, mass, and coupling constant of the black hole, as well as the rainbow function, \mathcal{F}_2 . In accordance with [28], the dyadosphere is a distinctive area enveloping the event horizon of an electrically charged black hole, wherein the strength of the electric field surpasses the crucial threshold required for the creation of particle pairs. Therefore, it is reasonable to expect that the energy density of the black hole, described by metric (3), is influenced by the energy of the test particle. Consequently, determining the form in which the energy of the particle is designated by the rainbow functions is of great significance. Although there are no experimental constraints on rainbow functions yet, there are different choices available in the literature (see [42] and references therein). In this context, Equation (21) yields different energy densities for the investigated black hole depending on the chosen form of the rainbow functions. Figs. 1 and 2 provide visual representations of the energy density, as given by Equation (21), with respect to r . As expected, Fig. 1 illustrates the considerably high energy density of the dyadosphere of a charged black hole in the RFG. Comparing Fig. 1 with Fig. 2, it can be

concluded that the energy density decreases for $\mathcal{F}_2 > 1$, whereas it increases for $0 < \mathcal{F}_2 < 1$. On the

other hand, the energy density for metric (2) was obtained by Xulu using Einstein $\left(\frac{4M}{r^3} - \frac{2Q^2}{r^4} + \frac{2Q^4\zeta}{5r^8}\right)$, Landau-Lifshitz $\left(\frac{Q^2}{8\pi r^4} + \frac{Q^4\zeta}{8\pi r^8}\right)$, Papapetrou $\left(\frac{Q^2}{8\pi r^4} + \frac{Q^4\zeta}{8\pi r^8}\right)$, and Weinberg $\left(\frac{Q^2}{8\pi r^4} + \frac{Q^4\zeta}{8\pi r^8}\right)$ formulations [34]. These results depend on the higher orders of $1/r$, as shown in Equation (21). This dependence supports the variation in energy density depicted in Figs. 1 and 2.

It is apparent from Equation (21) that the last term plays a crucial role in the dyadospheric region, which is characterized by small values of r . In addition, it is necessary to have $\zeta < 0$ in order to get real energy density.

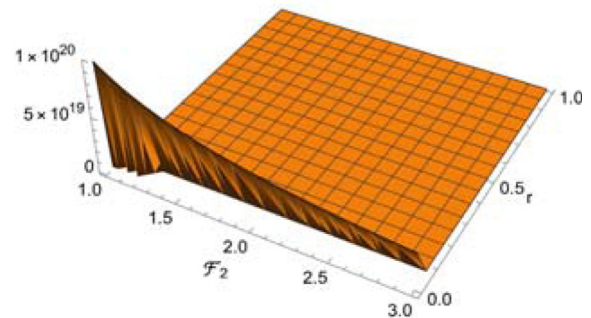


Fig. 1. Energy density vs (\mathcal{F}_2, r) with $M = 1, Q = 1, \zeta = -1$ and $\theta = \pi/2$ for $\mathcal{F}_2 > 1$.

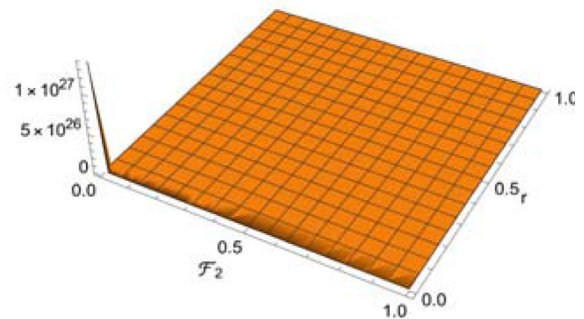


Fig. 2. Energy density vs (\mathcal{F}_2, r) with $M = 1, Q = 1, \zeta = -1$ and $\theta = \pi/2$ for $0 < \mathcal{F}_2 < 1$.

Furthermore, it is important to highlight that our obtained result (21) retrieves two distinct energy density expressions for black holes within the following limits.

i. $\zeta \rightarrow 0$ gives the Reissner-Nordström black hole

$$\chi_{NR} = \frac{\sin \theta}{8\pi \mathcal{F}_2} \left(\frac{\frac{2M}{r} - \frac{Q^2}{r^2}}{\sqrt{1 + \frac{Q^2}{r^2} - \frac{2M}{r}}} - \frac{\left(\frac{M}{r} - \frac{Q^2}{r^2}\right)^2}{\left(1 + \frac{Q^2}{r^2} - \frac{2M}{r}\right)^{3/2}} + 2\sqrt{1 + \frac{Q^2}{r^2} - \frac{2M}{r}} - 2 \right), \tag{24}$$

ii. $\zeta \rightarrow 0$ and $Q \rightarrow 0$ give the Schwarzschild black hole

$$\chi_S = \frac{\sin \theta}{8\pi \mathcal{F}_2} \left(\frac{\frac{2M}{r}}{\sqrt{1 - \frac{2M}{r}}} - \frac{\left(\frac{M}{r}\right)^2}{\left(1 - \frac{2M}{r}\right)^{3/2}} + 2\left(1 - \frac{2M}{r}\right)^{1/2} - 2 \right). \tag{25}$$

The present study has provided the first determination of the energy density of the dyadosphere of an energy-dependent charged black hole in the RFG from the perspective of quantum gravity. The energy density, as given by Equation (21) has been influenced by various factors, including the charge and mass of the black hole, coupling constant, and rainbow function \mathcal{F}_2 . It has been important to highlight that our obtained result (21) encompasses two distinct energy density expressions for black holes, with the limits $\zeta \rightarrow 0$ corresponding to the

Reissner-Nordström black hole, and $(\zeta, Q) \rightarrow 0$ corresponding to the Schwarzschild black hole.

This study presents a novel perspective for further research on the energy densities of black holes, encompassing both theoretical and experimental aspects, with significant implications in the field. Finally, it is worth emphasizing here that various models (see Table 1) of rainbow functions have been proposed in literature and our research can be further deepened by using these definitions.

Conflict of interest

The authors declare no conflict of interest.

Acknowledgments

We would like to thank TUBITAK (the Scientific and Technical Research Council of Turkey) for their valuable financial support.

References

- [1] A. Kempf, G. Mangano, R.B. Mann, Hilbert space representation of the minimal length uncertainty relation, Phys. Rev. D 52 (1995) 1108–1118, <https://doi.org/10.1103/PhysRevD.52.1108>.
- [2] L.J. Garay, Quantum gravity and minimum length, Int. J. Mod. Phys. A 10 (1995) 145–165, <https://doi.org/10.1142/S0217751X95000085>.
- [3] G. Amelino-Camelia, Doubly-special relativity: first results and key open problems, Int. J. Mod. Phys. D 11 (2002) 1643–1669, <https://doi.org/10.1142/S021827180200302X>.
- [4] C. Rovelli, Loop quantum gravity, Living Rev. Relat. 11 (2008) 5, <https://doi.org/10.12942/lrr-2008-5>.
- [5] A. Ashtekar, E. Bianchi, A short review of loop quantum gravity, Rep. Prog. Phys. 84 (2021) 042001, <https://doi.org/10.1088/1361-6633/abed91>.
- [6] F. Giacomini, C. Brukner, Quantum superposition of spacetimes obeys Einstein's equivalence principle, AVS Quantum Sci 4 (2022) 015601, <https://doi.org/10.1116/5.0070018>.
- [7] J. Foo, C.S. Arabaci, M. Zych, R.B. Mann, Quantum signatures of black hole mass superpositions, Phys. Rev. Lett. 129 (2022) 181301, <https://doi.org/10.1103/PhysRevLett.129.181301>.
- [8] S.H. Hendi, B.E. Panah, S. Panahiyan, Topological charged black holes in massive gravity's rainbow and their thermodynamical analysis through various approaches, Phys. Lett. B 769 (2017) 191–201, <https://doi.org/10.1016/j.physletb.2017.03.051>.
- [9] G. Amelino-Camelia, Relativity in spacetimes with short-distance structure governed by an observer-independent (Planckian) length scale, Int. J. Mod. Phys. D 11 (2002) 35–59, <https://doi.org/10.1142/S0218271802001330>.
- [10] J. Magueijo, L. Smolin, Lorentz invariance with an invariant energy scale, Phys. Rev. Lett. 88 (2002) 190403, <https://doi.org/10.1103/PhysRevLett.88.190403>.
- [11] C. Leiva, J. Saavedra, J. Villanueva, Geodesic structure of the Schwarzschild black hole in rainbow gravity, Mod. Phys. Lett. A 24 (2009) 1443–1451, <https://doi.org/10.1142/S0217732309029983>.
- [12] J. Magueijo, L. Smolin, Gravity's rainbow, Class. Quant. Grav. 21 (2004) 1725–1736, <https://doi.org/10.1088/0264-9381/21/7/001>.
- [13] P. Galan, G.A.M. Marugan, Entropy and temperature of black holes in a gravity's rainbow, Phys. Rev. D 74 (2006) 044035, <https://doi.org/10.1103/PhysRevD.74.044035>.

Table 1. Most used rainbow functions.

Classes	Definitions ^a			Reference
	\mathcal{F}_1	\mathcal{F}_2		
Class I	$(b_1 \xi)^{-1} (e^{b_1 \xi} - 1)$	1		[10]
	$(1 - b_2 \xi)^{-1}$	1		[21]
	$\sqrt{e^{-\xi^2}}$	1		[22]
Class II	$\sqrt{1 - \xi^2}$	1		[16]
	1	$1 + \frac{\xi}{2}$		[11]
	1	$\sqrt{1 - b_3 \xi^{b_1}}$		[43]
Class III	1	$1 + \xi^{b_5}$		[44]
	$1 + \frac{\xi}{2}$	$1 + \frac{\xi}{2}$		[11]
	$(1 + b_6 \xi)^{-1}$	$(1 + b_6 \xi)^{-1}$		[10]

^a The free model parameters are denoted as b_i ($i = 1, 2, 3, 4, 5, 6$).

- [14] R. Garattini, Gravity's rainbow and black hole entropy, *J. Phys. Conf. Ser.* 942 (2017) 012011, <https://doi.org/10.1088/1742-6596/942/1/012011>.
- [15] T. Roy, U. Debnath, Entropy bound and EGUP correction of d-dimensional Reissner–Nordström black hole in rainbow gravity, *Int. J. Mod. Phys. A* 38 (2023) 2350034, <https://doi.org/10.1142/S0217751X23500343>.
- [16] Y. Ling, X. Li, H. Zhang, Thermodynamics of modified black holes from gravity's rainbow, *Mod. Phys. Lett. A* 22 (2007) 2749–2756, <https://doi.org/10.1142/S0217732307022931>.
- [17] S.H. Hendi, M. Faizal, B.E. Panah, S. Panahiyan, Charged dilatonic black holes in gravity's rainbow, *Eur. Phys. J. C* 76 (2016) 296, <https://doi.org/10.1140/epjc/s10052-016-4119-4>.
- [18] J.W. Kim, S.K. Kim, Y.J. Park, Thermodynamic stability of modified Schwarzschild-AdS black hole in rainbow gravity, *Eur. Phys. J. C* 76 (2016) 557, <https://doi.org/10.1140/epjc/s10052-016-4393-1>.
- [19] B.E. Panah, Effects of energy dependent spacetime on geometrical thermodynamics and heat engine of black holes: gravity's rainbow, *Phys. Lett. B* 787 (2018) 45–55, <https://doi.org/10.1016/j.physletb.2018.10.042>.
- [20] B. Hamil, B.C. Lütfüoğlu, Thermodynamics of Schwarzschild black hole surrounded by quintessence in gravity's rainbow, *Nucl. Phys. B* 990 (2023) 116191, <https://doi.org/10.1016/j.nuclphysb.2023.116191>.
- [21] Z.W. Feng, S.Z. Yang, Thermodynamic phase transition of a black hole in rainbow gravity, *Phys. Lett. B* 772 (2017) 737–742, <https://doi.org/10.1016/j.physletb.2017.07.057>.
- [22] C.Z. Liu, J.Y. Zhu, Hawking radiation and black hole entropy in a gravity's rainbow, *Gen. Relat. Gravit.* 40 (2008) 1899–1911, <https://doi.org/10.1007/s10714-008-0607-7>.
- [23] A.F. Ali, Black hole remnant from gravity's rainbow, *Phys. Rev. D* 89 (2014) 104040, <https://doi.org/10.1103/PhysRevD.89.104040>.
- [24] A.F. Ali, M. Faizal, B. Majumder, Absence of an effective horizon for black holes in gravity's rainbow, *Europhys. Lett.* 109 (2015) 20001, <https://doi.org/10.1209/0295-5075/109/20001>.
- [25] Y. Gim, W. Kim, Black hole complementarity in gravity's rainbow, *J. Cosmol. Astropart. Phys.* 5 (2015) 2, <https://doi.org/10.1088/1475-7516/2015/05/002>.
- [26] M. Khodadi, K. Nozari, H.R. Sepangi, More on the initial singularity problem in gravity's rainbow cosmology, *Gen. Relat. Gravit.* 48 (2016) 166, <https://doi.org/10.1007/s10714-016-2160-0>.
- [27] S. Hawking, Black holes and thermodynamics, *Phys. Rev. D* 13 (1976) 191–197, <https://doi.org/10.1103/PhysRevD.13.191>.
- [28] R. Ruffini, The dyadosphere of black holes and gamma-ray bursts, *Astron. Astrophys., Suppl. Ser.* 138 (1999) 513–514, <https://doi.org/10.1051/aas:1999331>.
- [29] R. Ruffini, in: H. Salto, eds., *On the Dyadosphere of Black Holes*, XLIX Yamada Conference on Black Holes and High-Energy Astrophysics, Univ. Acad. Press, Tokyo, 1998, <https://doi.org/10.48550/arXiv.astro-ph/9811232>.
- [30] G. Preparata, R. Ruffini, S.S. Xue, The dyadosphere of black holes and gamma-ray bursts, *A&A* 338 (1998) L87–L90, <https://doi.org/10.48550/arXiv.astro-ph/9810182>.
- [31] V.A. de Lorenci, N. Figueredo, H.H. Fliche, M. Novello, Dyadosphere bending of light, *A&A* 369 (2001) 690–693, <https://doi.org/10.1051/0004-6361:20010089>.
- [32] F. Rahaman, M. Kalam, K.A. Rahman, Thin shell wormhole due to dyadosphere of a charged black hole, *Mod. Phys. Lett. A* 24 (1) (2009) 53–61, <https://doi.org/10.1142/S0217732309027406>.
- [33] O. Aydogdu, M. Salti, Møller's energy in the dyadosphere of a charged black hole, *Pramana* 67 (2006) 239–247, <https://doi.org/10.1007/s12043-006-0068-z>.
- [34] S.S. Xulu, Energy distribution in the dyadosphere of a charged black hole, arXiv: gr-qc/0304081, <https://doi.org/10.48550/arXiv.gr-qc/0304081>.
- [35] I. Radinschi, KKW analysis for the dyadosphere of a charged black hole, arXiv: gr-qc/0511142, <https://doi.org/10.48550/arXiv.gr-qc/0511142>.
- [36] A. Einstein, Riemann-geometrie mit aufrechterhaltung des begriffes des fernparallelismus, *Preussische Akademie der Wissenschaften, Phys.-math. Klasse, Sitzungsberichte* (1928), <https://doi.org/10.1002/3527608958.ch36>.
- [37] J.W. Maluf, J.F. da Rocha-Neto, T.M.L. Toribio, K.H. Castello-Branco, Energy and angular momentum of the gravitational field in the teleparallel geometry, *Phys. Rev. D* 65 (2002) 124001, <https://doi.org/10.1103/PhysRevD.65.124001>.
- [38] T. Vargas, The energy of the universe in teleparallel gravity, *Gen. Relat. Gravit.* 36 (2004) 1255–1264, <https://doi.org/10.1023/B:GERG.0000022386.29438.be>.
- [39] H. Abedi, M. Salti, Multiple field modified gravity and localized energy in teleparallel framework, *Gen. Relat. Gravit.* 47 (2015) 93, <https://doi.org/10.1007/s10714-015-1935-z>.
- [40] M. Salti, I. Acikgoz, Black holes, wormholes and the Hamiltonian approach in the framework of teleparallel gravity, *Phys. Scripta* 87 (2013) 045006, <https://doi.org/10.1088/0031-8949/87/04/045006>.
- [41] K. Hayashi, T. Shirafuji, Energy, momentum and angular momentum in Poincaré gauge theory, *Prog. Theor. Phys.* 73 (1985) 54–74, <https://doi.org/10.1143/PTP.73.54>.
- [42] O. Aydogdu, M. Salti, Gravitational waves in f(R, T)-rainbow gravity: even modes and the Huygens principle, *Phys. Scripta* 97 (2022) 125013, <https://doi.org/10.1088/1402-4896/aca0cc>.
- [43] U. Jacob, F. Mercati, G. Amelino-Camelia, T. Piran, Modifications to Lorentz invariant dispersion in relatively boosted frames, *Phys. Rev. D* 82 (2010) 084021, <https://doi.org/10.1103/PhysRevD.82.084021>.
- [44] Z. Amirabi, M. Halilsoy, S.H. Mazharimousavi, Thin-shell wormholes in rainbow gravity, *Mod. Phys. Lett. A* 33 (2018) 1850049, <https://doi.org/10.1142/S0217732318500499>.